Inorg. Chem. **2008**, *47*, 4356−4367

Imidazole Substituent Effects on Oxidative Reactivity of Tripodal(imid)$_2$(thioether)Cu^I Complexes

Lei Zhou and Kenneth M. Nicholas*

Department of Chemistry and Biochemistry, University of Oklahoma, Norman, Oklahoma 73019

Received January 2, 2008

In the search for new bis(imidazole)thioether (BIT) copper complexes that accurately mimic the electronic and reactivity features of the Cu$_M$ site of copper hydroxylase enzymes, a set of tripodal BIT ligands **4a**,**b**−**6a**,**b** has been synthesized that vary according to the imidazole *C*-(Ph or H) and *N*-(H or Me) substituents, as well as the position (2- or 4-) of the tripodal attachment. Corresponding [(BIT)Cu(L)](PF$_6$) complexes **7a**,**b′**, **8a**,**b′**, and **9a′**,**b′** [L = CO (**a**), CH$_3$CN (**b**)] have been prepared and characterized spectroscopically. The IR spectra of **7a**−**9a** (L = CO), specifically ν(CO), show little variation (2090–2100 cm^{-1}), suggesting a similar electronic character of the Cu centers. In contrast, cyclic voltammetric analysis of these compounds (L = CH$_3$CN) reveals quasi-reversible oxidation waves with significant variation of E_{pa} in the range of + 0.45–0.57 V vs Fc/Fc$^+$, depending on the imidazole substituents. Each of the [(BIT)Cu(CH$_3$CN)]PF$_6$ complexes reacts with dioxygen to form [(BIT)Cu$^{II}_2$(μ-OH)$_2$](PF$_6$)$_2$ derivatives, **10**−**12**, but they vary considerably in their relative reactivity, following the same trend as the ease of their electrochemical oxidation, that is, [(2-BIT^{NMe})Cu(CH$_3$CN)]$^+$ (**9b′**) > [(4-BIT^{Ph,NMe})Cu(CH$_3$CN)]$^+$ (**8b′**) > [(2-BIT^{Ph2,NMe})Cu(CH$_3$CN)]$^+$ (**1a′**) > [(4-BIT^{Ph,NH})Cu(CH$_3$CN)]$^+$ (**7b′**). Thus, *N*-Me substitution and 4-tethering on the imidazole unit increase oxidation and oxygenation reactivity, while Ph-substitution and 2-tethering decrease reactivity. PM3 and DFT calculations are employed to analyze the relative stability, the electronic features, the Cu−CO vibrtional frequency, and the electrochemical and oxidative reactivity of the complexes.

Introduction

The copper hydroxylase enzymes, dopamine β-hydroxylase (DβH,) and peptidylglycine α-hydroxylating monooxygenase (PHM), catalyze the regio- and enantioselective hydroxylation of somewhat activated C−H bonds by dioxygen.[1] The enzymes apparently have very similar active site structures, featuring two Cu centers separated by 12 Å, the Cu$_H$ (Cu$_A$) site being ligated to three histidine-derived imidazoles and the Cu$_M$ (Cu$_B$) site by two histidines and a methionine residue (Figure 1).[2] Spectroscopic and amino acid mutagenesis studies suggest that upon reduction both dioxygen and the substrate are activated at the Cu$_M$ site and that the Cu$_H$ site serves as an electron transfer shuttle from the ascorbate reductant to the Cu$_M$ site.[3] A recent X-ray structure of the O$_2$-bound PHM enzyme has revealed a rare end-on

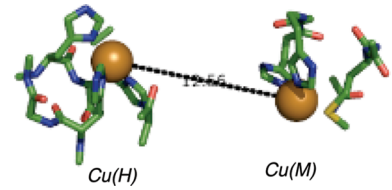

Figure 1. Cu-hydroxylase active site.

coordination mode to the Cu$_M$ center,[4–6] contrasting with the more common side-on mononuclear and bridging bimetallic bonding modes found in most synthetic complexes and in

* To whom correspondence should be addressed. E-mail: knicholas@ou.edu.

(1) (a) Klinman, J. P. *Chem. Rev.* **1996**, *96*, 2541–2562. (b) Lewis, E. A.; Tolman, W. B. *Chem. Rev.* **2004**, *104*, 1047–1076.
(2) Prigge, S. T.; Mains, R. E.; Amzel, L. M. *Science* **1997**, *278*, 1300–1305.
(3) (a) Prigge, S. T.; Mains, R. E.; Eipper, B. A.; Amzel, L. M. *Cell. Mol. Life Sci.* **2000**, *57*, 1236–1259. (b) Prigge, S. T.; Kolhekar, A. S.; Eipper, B. A.; Mains, R. E.; Amzel, L. M. *Nat. Struct. Biol.* **1999**, *6*, 976–983. (c) Evans, J. P.; Ahn, K.; Klinman, J. P. *J. Biol. Chem.* **2003**, *278*, 49691–49698. (d) Chen, P.; Solomon, E. I. *J. Am. Chem. Soc.* **2004**, *126*, 4991–5000.
(4) Prigge, S. T.; Eipper, B. A.; Mains, R. E.; Amzel, L. M. *Science* **2004**, *304*, 864–867.
(5) Chaudhuri, P.; Hess, M.; Weyhermuller, T.; Wieghardt, K. *Angew. Chem., Int. Ed.* **1999**, *38*, 1095–1098.
(6) Wurtele, C.; Gaoutchenova, E.; Harms, K.; Holthausen, M. C.; Sundermeyer, J.; Schindler, S. *Angew. Chem., Int. Ed.* **2006**, *45*, 3867–3869.

10.1021/ic800007t CCC: $40.75
Published on Web 04/10/2008

the O_2-binding Cu-protein hemocyanin.[7] The mechanistic details of the substrate hydroxylation are unclear, but rate-limiting C−H bond-breaking with a significant tunneling component by a Cu-oxygen species is supported by the large intrinsic primary D-isotope effect (10.6) for both DβH and PHM.[8] Recent computational studies suggest that either a side-on Cu-superoxo[9] or a Cu-oxo species[10] is the likely H-abstracting agent.

Although many synthetic model complexes for these (and other) copper enzymes have been prepared with a variety of polydentate amine-, pyridine-, and pyrazolyl-based ligands,[7] remarkably few have incorporated the biologically most relevant imidazole (from histidine) donors.[11,12] Because of the significantly different basicity (pK_a imidazolium, 6.8; pyrazolium, 2.6; pyridinium, 5.2, tertiary ammonium, 9–10)[13] and donor/acceptor properties[14] of imidazole vis a vis the other common nitrogen ligands, we propose that the most accurate functional mimics for histidine-rich metalloenzymes will be provided by incorporation of the actual biological donor set. Regarding imidazole-based models for the Cu_H site, Sorrell and co-workers first reported copper(I) complexes of tripodal tris(*N*-methyl-2-imidazolyl)carbinol[12a] and tris(2-imidazolyl)phosphines.[12d] Dinuclear complexes of the former ligand, $[(tripod)_2Cu^I_2]Z_2$, are unreactive toward dioxygen, whereas a mononuclear Cu^I-complex of the latter ligand reacts with dioxygen to produce a peroxodicopper(II) adduct. We recently investigated the chemistry of Cu^I complexes of the related, sterically demanding tripodal *tris*-(*N*-methyl-4,5-diphenyl-imidazolyl)methane ligands.[15] While these also form dinuclear Cu_2L_2-type complexes, mononuclear adducts $[(imid_3CR)CuL]Z$ are produced with L= acetonitrile, carbon monoxide, and *t*-BuNC. Reactions of dioxygen with these dinuclear complexes are sluggish, producing from the latter $[(imid)_3CH]Cu^{II}(acetone)(H_2O)]Z_2$.

Few complexes have been reported that possess the (amine)$_2$thioether coordination sphere relevant to the Cu_M site of the copper hydroxylases. Karlin and co-workers recently described Cu^{I,II} complexes of (non-imidazole) tridentate (pyridine)(amine)(thioether) ligands; oxygenation of $[(N_2S)Cu^I]^+$ at room temperature leads to ligand sulfoxidation, demonstrating O_2 activation and an oxygenation pathway not displayed by the enzymes.[16] They also reported a N_3S-thioether-Cu(I) complex that undergoes low temperature oxygenation to form a spectroscopically characterized end-on peroxodicopper(II) derivative.[17] Electrochemical studies of these systems found that the more easily oxidized complexes were also more reactive toward dioxygen. A few Cu^{II} complexes with mixed polydentate *imidazole*/thioether ligands have been characterized,[11] but until our recent studies, only one such Cu^I derivative had been reported.[11] In recent reports, we disclosed the preparation of tripodal *bis*-(4,5-diphenyl-2-imidazolyl)thioether (2-BIT$^{Ph2,SR,OH(Me)}$) ligands and the corresponding Cu(I) complexes, [(2-BIT$^{Ph2,SMe,OH(Me)}$)Cu(L)]PF_6 [L= CO (**1a**), CH_3CN (**1a′**)]. The IR ν(CO) absorptions of the $[(2\text{-BIT}^{Ph2,SMe})\text{Cu-CO}]^+$ complexes **1a** were found to be very similar to the enzymes $Cu_{(M)}$−CO, suggesting close electronic similarity of the synthetic and natural Cu centers.[19] In contrast to the enzymes, oxygenation of **1a′** affords a binuclear Cu(II)−hydroxo complex, $[(2\text{-BIT}^{Ph2,SMe})_2Cu_2(\mu\text{-OH})_2](OTf)_2$ (**2a**). Copper(I) complexes of the sterically hindered 2-BIT$^{Ph2,SR'}$ ligands **1b′** (R′= *t*-Bu) and **1c′** (R'= CPh_3) were found to undergo oxygenation by contrasting pathways.[20] The former (**1b′**) reacts slowly relative to **1a′**, producing two $(2\text{-BIT}^{Ph2,SBu\text{-}t})_2Cu_2(\mu\text{-OH})_2$-type complexes, **2b** + **2b′**, the latter of which is ortho-oxygenated on a neighboring aryl group (Scheme 1). On the other hand, oxygenation of the Cu^I complex derived from 2-BIT^{Ph2,SCPh3} (**1c′**) produced a novel dinuclear disulfide complex, $[(BIT^S)_2Cu_2(\mu\text{-OH})_2](PF_6)_2$ (**2c**).

Although the bis(imidazole)(thioether)Cu complexes investigated to date more accurately represent the donor ligand set of the Cu_M enzyme site than do non-imidazole N_2S ligands, significant differences between the active site models and enzymatic systems still exist. In addition to the C−Ar and N-Me groups of the synthetic ligands, which are absent

(7) (a) Mirica, L. M.; Ottenwaelder, X.; Stack, T. D. P. *Chem. Rev.* **2004**, *104*, 1013–1045. (b) Lewis, E. A.; Tolman, W. B. *Chem. Rev.* **2004**, *104*, 1047–1076. (c) Fujisawa, K.; Tanaka, M.; Moro-oka, Y.; Kitajima, N. *J. Am. Chem. Soc.* **1994**, *116*, 12079–12080. (d) Kitajima, N.; Fujisawa, K.; Fujimoto, C.; Morooka, Y.; Hashimoto, S.; Kitagawa, T.; Toriumi, K.; Tatsumi, K.; Nakamura, A. *J. Am. Chem. Soc.* **1992**, *114*, 1277–91. (e) Hatcher, L. Q.; Karlin, K. D. *J. Biol. Inorg. Chem.* **2004**, *9*, 669–683. (f) Hatcher, L. Q.; Vance, M. A.; Sarjeant, A. A. N.; Solomon, E. I.; Karlin, K. D. *Inorg. Chem.* **2006**, *45*, 3004–3013. (g) Aboelella, N. W.; Kryatov, S. V.; Gherman, B. F.; Brennessel, W. W.; Young, V. G.; Sarangi, R.; Rybak-Akimova, E. V.; Hodgson, K. O.; Hedman, B.; Solomon, E. I.; Cramer, C. J.; Tolman, W. B. *J. Am. Chem. Soc.* **2004**, *126*, 16896–16911. (h) Itoh, S.; Fukuzumi, S. *Bull. Chem. Soc. Jpn.* **2002**, *75*, 2081–2095.

(8) (a) Takahashi, K.; Onami, T.; Noguchi, M. *Biochem. J.* **1998**, *336*, 131–137. (b) Francisco, W. A.; Merkler, D. J.; Blackburn, N. J.; Klinman, J. P. *Biochemistry* **1998**, *37*, 8244–8252. (c) Miller, S. M.; Klinman, J. P. *Biochemistry* **1985**, *24*, 2114–2127. (d) Klinman, J. P.; Humphries, H.; Voet, J. G. *J. Biol. Chem.* **1980**, *255*, 11648–11651.

(9) Chen, P.; Solomon, E. I. *J. Am. Chem. Soc.* **2004**, *126*, 4991–5000.

(10) (a) Kamachi, T.; Kihara, N.; Shiota, Y.; Yoshizawa, K. *Inorg. Chem.* **2005**, *44*, 4226–4236. (b) Yoshizawa, K.; Kihara, N.; Kamachi, T.; Shiota, Y. *Inorg. Chem.* **2006**, *45*, 3034–3041.

(11) Cao, Y. D.; Zheng, Q. Y.; Chen, C. F.; Hu, H. M.; Huang, Z. T. *Inorg. Chim. Acta* **2004**, *357*, 316–320.

(12) (a) Sorrell, T. N.; Borovik, A. S. *J. Am. Chem. Soc.* **1987**, *109*, 4255–4260. (b) Tang, C. C.; Davalian, D.; Huang, P.; Breslow, R. *J. Am. Chem. Soc.* **1978**, *100*, 3918–3922. (c) Breslow, R.; Hunt, J. T.; Smiley, R.; Tarnowski, T. *J. Am. Chem. Soc.* **1983**, *105*, 5337–5342. (d) Sorrell, T. N.; Allen, W. E.; White, P. S. *Inorg. Chem.* **1995**, *34*, 952–960.

(13) Bruice, P. Y. *Organic Chemistry*, 4th ed.; Prentice-Hall: Trenton, NJ, 2004; pp A8–9.

(14) (a) Marques, H. M.; Munro, O. Q.; Munro, T.; Wet, M. D.; Vashi, P. R. *Inorg. Chem.* **1999**, *38*, 2312–2319. (b) Johnson, C. R.; Henderson, W. W.; Shepherd, R. E. *Inorg. Chem.* **1984**, *23*, 2754–2763. (c) Peters, L.; Hubner, E.; Burzlaff, N. *J. Organomet. Chem.* **2005**, *690*, 2009–2016.

(15) Zhou, L.; Powell, D.; Nicholas, K. M. *Inorg. Chem.* **2007**, *46*, 2316–2321.

(16) Lee, Y.; Lee, D.-H.; Narducci-Sarjeant, A. A.; Zakharov, L. N.; Rheingold, A. L.; Karlin, K. D. *Inorg. Chem.* **2006**, *45*, 10098–10107.

(17) Hatcher, L. Q.; Lee, D.-H.; Vance, M. A.; Milligan, A. E.; Sarangi, R.; Hodgson, K. O.; Hedman, B.; Solomon, E. I.; Karlin, K. D. *Inorg. Chem.* **2006**, *45*, 10055–10057.

(18) (a) Tran, K. C.; Battioni, J. P.; Zimmermann, J. L.; Bois, C.; Koolhaas, G. J. A. A.; Leduc, P.; Mulliez, E.; Boumchita, H.; Reedijk, J.; Chottard, J. C. *Inorg. Chem.* **1994**, *33*, 2808–2814. (b) Zoeteman, M.; Bouwman, E.; De Graff, R. A. G. D.; Driessen, W. L.; Reedijk, J.; Zanello, P. *Inorg. Chem.* **1990**, *29*, 3487–3492. (c) Dagdigian, J. V.; Reed, C. A. *Inorg. Chem.* **1979**, *18*, 2623–2626.

(19) Zhou, L.; Powell, D.; Nicholas, K. M. *Inorg. Chem.* **2006**, *45*, 3840–3842.

(20) Zhou, L.; Powell, D.; Nicholas, K. M. *Inorg. Chem.* **2007**, *46*, 7789–7799.

Scheme 1

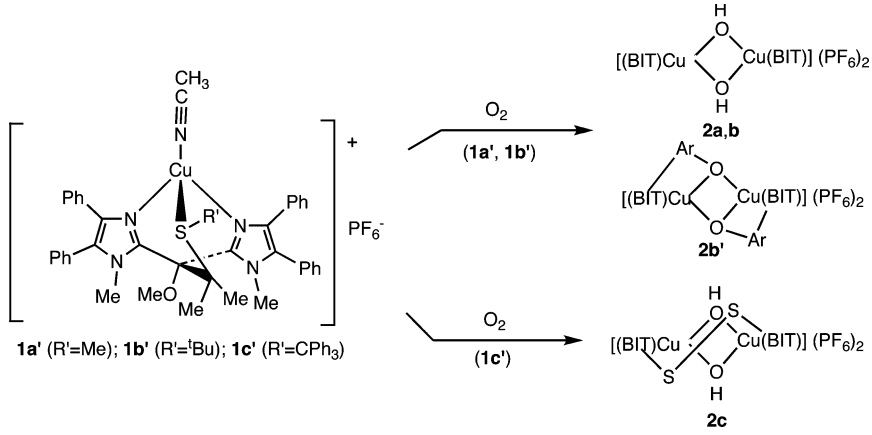

in the protein-derived imidazole from histidine, the tripodal alkyl tether is attached at C-2 for the synthetic N_2S complexes while the histidine-derived imidazole is alkyl-substituted at C-4,5. What effects will such differences have on the electronic character and, particularly, the reactivity of the respective metal centers? While the steric and electronic effects of the type of C- and N-substitution could perhaps be qualitatively anticipated, the effects of the C-2 versus C-4,5 position of substitution are less obvious. A study by Breslow and co-workers[21] showed that $[(4\text{-imid})_3\text{COH}]M^{II}$ complexes are significantly more stable (K_a is $\sim 10^2$ greater) than the $[(2\text{-imid})_3\text{COH}]M^{II}$. What would be the impact of such substitutional differences on the (BIT)Cu$-$$O_2$ reactivity? In the present report, we address these questions with the preparation of a new set of $(imid)_2$(thioether)Cu^I complexes and investigate their electronic characteristics through spectroscopic characterization of their CO adducts, their electrochemical redox behavior and reactivity toward dioxygen, and computational studies.

Scheme 2

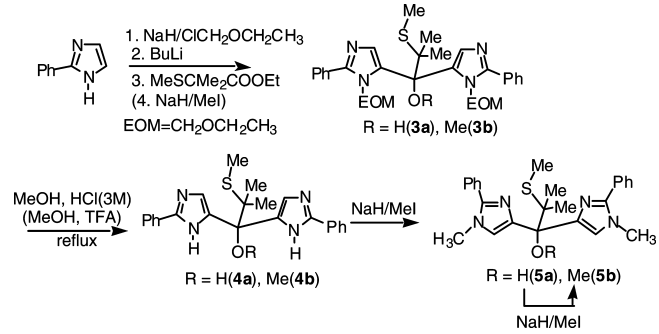

Scheme 3

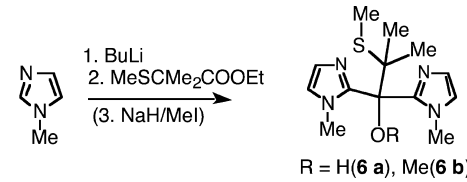

Results

Ligand Synthesis. The abbreviated general formula for the bis-imidazole-thioether (BIT) ligands prepared is: #-$BIT^{\#\text{-R,NR,SMe,OR}}$, sequentially indicating the position of tripodal attachment, and the imidazole (to C, N), the thioether, and the tripodal C-substituents, respectively. In all of the present set of ligands and complexes the thiomethyl unit is present so the SMe superscript will be omitted for brevity. To prepare 4-tethered ligands the conveniently introduced and removed ethoxymethyl (EOM) group was employed to direct imidazole lithiation/alkylation at the 4-position[22] and to enable easy removal. The EOM-protected compounds 5-$BIT^{2\text{-Ph,NEOM,OH(Me)}}$ (**3a**, **3b**) were thus prepared by double addition of lithiated *N*-EOM-imidazole to the ester $MeSCMe_2CO_2Et$ (57% from 2-Ph-1-EOM-imidazole to alcohol, **3a**), followed by O-methylation under basic conditions (Scheme 2). The EOM-protected tripodal compounds **3a** and **3b** were converted into the *N*-H derivatives 5-$BIT^{2\text{-Ph,NH,OH(Me)}}$ (**4a**, **4b**) by refluxing in acidic MeOH solution. Alcohol **4a** was converted into *N*-methylated tripod 4-$BIT^{2\text{-Ph,NMe,OH}}$ (**5a**) (41%) and methoxy compound 4-$BIT^{2\text{-Ph,NMe,OMe}}$ (**5b**) was produced from **5a** (70%) by reaction with NaH/MeI. A new pair of N_2S-ligands 2-$BIT^{\text{NH,OH(Me)}}$ (**6a**, **6b**), lacking aryl groups and tethered at the C-2 position, was also efficiently prepared by addition of 2-lithio-*N*-methyl imidazole to the thioether ester (Scheme 3), followed by *O*-alkylation for the preparation of **6b**. All of the ligands thus produced were characterized spectroscopically and were obtained in an analytically pure form.

Preparation and IR spectra of N_2S-Tripod Cu(I)$-$Carbonyl Complexes. The IR Cu$-$CO vibrational frequency, affected by the balance between σ-CO-to-Cu donation and Cu-to-CO π^* backbonding, has been considered to be a measure of the electronic character of the Cu center of LCu$-$CO complexes.[23] In addition, metal–carbonyl derivatives have been used as models to gauge M$-$$O_2$ complex formation/stability.[24] To use this probe to detect electronic differences among the various imidazole-substituted ligands,

(21) Tang, C. C.; Davalian, D.; Huang, P.; Breslow, R. *J. Am. Chem. Soc.* **1978**, *100*, 3918–3922.

(22) Breslow, R.; Hunt, J. T.; Smiley, R.; Tarnowski, T. *J. Am. Chem. Soc.* **1983**, *105*, 5337–5342.

(23) (a) Imai, S.; Fujisawa, K.; Kobayashi, T.; Shirasawa, N.; Fujii, H.; Yoshimura, T.; Kitajima, N.; Moro-oka, Y. *Inorg. Chem.* **1998**, *37*, 3066–3070. (b) Kujime, M.; Kurahashi, T.; Tomura, M.; Fujii, H. *Inorg. Chem.* **2007**, *46*, 541–551.

Scheme 4

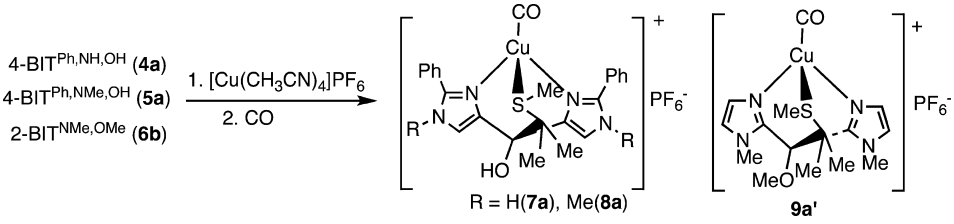

Table 1. Summary of IR, CV, and Oxygen Reactivity of [BIT)CuL]$^+$ Complexes **1a′**, **7′–9′**

[(BIT)CuL]PF$_6$ complex	IR ν_{CuCO} (cm^{-1})^a (L = CO) **1a**, **7a–9a**	CV E_{pa} (mV)^b (L = CH_3CN) **1a′**, **7b′−9b′**	O_2 reactivity (L = CH_3CN) **1a′**, **7b′−9b′**
[(2-BIT$^{Ph2,NMe,OHMe)}$)Cu(L)]$^+$ (**1a**,**1a′**)	2097	+ 0.54 V	2 h at rt
[(4-BIT$^{Ph,NH,OHMe)}$)Cu(L)]$^+$ (**7a**,**7b′**)	2094	+ 0.57 V	12 h at rt
[(4-BIT$^{Ph,NMe,OHMe)}$)Cu(L)]$^+$ (**8a**,**8b′**)	2094	+ 0.51 V	5 min at −50 °C
[(2-BIT$^{NMe,OHMe)}$)Cu(L)]$^+$ (**9a′**,**9b′**)	2105	+ 0.45 V	2 min at −70 °C

^{a} KBr pellet. ^{b} Pt working and auxiliary electrodes and Ag/AgCl reference electrodes: CH_2Cl_2,Bu_4NPF_6, $E_{pa} - E_{1/2}(Cp_2Fe)$; 1 atm O_2, CH_2Cl_2 solvent.

we prepared three new copper−carbonyl complexes, **7a**, **8a**, and **9a′**, via reactions of the respective ligands **4a**, **5a**, and **6b** with [Cu(CH$_3$CN)$_4$]PF$_6$, followed by exposure of the intermediate [(BIT)Cu(CH$_3$CN)]PF$_6$ species (not isolated) to carbon monoxide (Scheme 4). The CO adducts **7a**−**9a′** were isolated by ether precipitation and characterized by NMR, ESI-MS, and IR spectroscopy. The IR Cu−CO vibrational frequencies of these compounds, together with that of the previously prepared 2-tethered-4,5-diphenylated derivative **1a**, are listed in Table 1. It can be seen that these vary only by ±10 cm^{-1}, revealing no systematic trend nor significant effects of replacing C−Ph for C−H, *N*-Me/H, or 2/4-tethered tripodal substitution.

Cyclic Voltammetry. To further probe the electronic characteristics of the various [N_2S-Cu(CH$_3$CN)]PF$_6$ complexes, cyclic voltammetry studies were carried out. The complexes **1a′**, **7b′**, **8b′**, and **9b′** (L = CH$_3$CN) for CV analysis were produced in situ by combination of the respective BIT^{OMe} ligands with [Cu(CH$_3$CN)$_4$]PF$_6$ (1:1) in CH_2Cl_2 solution (1.0 mM) under nitrogen with 0.1 M NBu_4PF_6 as the supporting electrolyte. Electrochemical oxidation/reduction was effected by Pt (working /auxiliary) and Ag/AgCl reference electrodes with final referencing to added ferrocene$^{(o,+)}$. The phenylated complexes **1a′**, **7b′**, and **8b′** exhibit quasireversible oxidation waves (Cu$^{I/II}$) with the return reduction peak having a lower current and separated from the oxidation peak by 150–190 mV. Oxidation of the non-Ph complex **9b′** was essentially irreversible ($E_{pa} - E_{pc} \approx 600$ mV). Therefore, the potentials reported are based on the oxidation peak, E_{pa}, relative to $E_{1/2}$ for Cp_2Fe oxidation (Table 1).[16,25] From these data, it is seen that the ease of oxidation is in the order **9b′** > **8b′** > **1a′** > **7b′**. Thus the 4-tethered-Ph-complex **8b′** is more easily oxidized than the 2-tethered Ph$_2$-derivative **1a′**; the *N*-Me derivative **8b′** easier than the *N*-H complex **7b′**; and the 2-tethered non-Ph complex **9b′** is more easily oxidized than the 2-BIT^{Ph2} complex **1a′**.

Scheme 5.

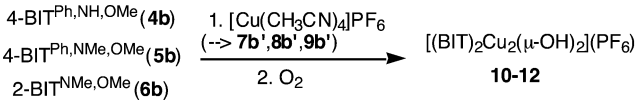

Dioxygen Reactivity. To evaluate the reactivity of these various complexes with dioxygen the Cu complexes of the 4-tethered BIT^{Ph,NH,OMe} (**7b′**), BIT^{Ph,NMe,OMe} (**8b′**), and 2-tethered BIT^{NMe,OMe} (**9b′**) ligands were generated under argon at low temperature by combining [Cu(CH$_3$CN)$_4$]PF$_6$ with the corresponding BIT ligand (1:1) in CH_2Cl_2, followed by exposure to dry dioxygen (1 atm). Oxygenation was signaled by a change in the solution color from nearly colorless/light yellow (Cu^I) to green or blue (Cu^{II}), characteristic of the hydroxo dimer complexes, [(BIT)$_2$Cu$_2$(OH)$_2$](PF$_6$)$_2$ (**10**−**12**, vide infra, Scheme 5.). If no change was observed after a few hours at −60 °C, the reaction mixture was allowed to warm to room temperature over several hours. In no case was a distinct transient color observed that would suggest appreciable buildup of an intermediate complex, for example, [(BIT)Cu(O$_2$)]$^+$. Importantly, the four complexes **1a′**, **7b′**, **8b′**, and **9b′** react at remarkably different rates. Thus, the oxygenation reactions of the 4-tethered-2-Ph-NMe complex **8b′** and the 2-tethered non-Ph complex **9b′** changed color *within minutes at −50 °C*, while 4-BIT$^{2\text{-}Ph,NH}$ complex **7b′**, similar to the original 2-BIT^{Ph2,NMe} derivative **1a′**, reacts with O_2 only slowly upon warming to *room temperature over 2–12 h*. The relative reactivity of **1a′** and **7b′**−**9b′** toward dioxygen thus parallels their ease of electrochemical oxidation.

The hydroxo dimers, [L$_2$Cu$_2$(OH)$_2$](PF$_6$)$_2$ **10**−**12**, were isolated in 60–70% yield upon ether diffusion into the reaction mixtures. These complexes were identified by the presence of appropriate molecular ions in their ESI-mass spectra with the Cu$_2$ isotopic signature, IR spectra (ν_{OH} at 3390–3430 cm^{-1}), and electronic spectra (327–370 and 540 nm). The structural assignments were confirmed by X-ray diffraction of each complex, Figures 2−4. The two Ph-

(24) (a) Kretzer, R. M.; Ghiladi, R. A.; Lebeau, E. L.; Liang, H.-C.; Karlin, K. D. *Inorg. Chem.* **2003**, *42*, 3016–3025. (b) Karlin, K. D.; Tyeklar, Z.; Farooq, A.; Haka, M. S.; Ghosh, P.; Cruse, R. W.; Gultneh, Y.; Hayes, J. C.; Toscano, P. J.; Zubieta, J. *Inorg. Chem.* **1992**, *31*, 1436–1451. (c) Nelson, S. M.; Lavery, A.; Drew, M. G. B. *J. Chem. Soc., Dalton Trans.* **1986**, *5*, 911–920.

(25) (a) Hatcher, L. Q.; Vance, M. A.; Narducci Sarjeant, A. A.; Solomon, E. I.; Karlin, K. D. *Inorg. Chem.* **2006**, *45*, 3004–3013. (b) Fujisawa, K.; Ono, T.; Ishikawa, Y.; Amir, N.; Miyashita, Y.; Okamoto, K.-I.; Lehnert, N. *Inorg. Chem.* **2006**, *45*, 1698–1713.

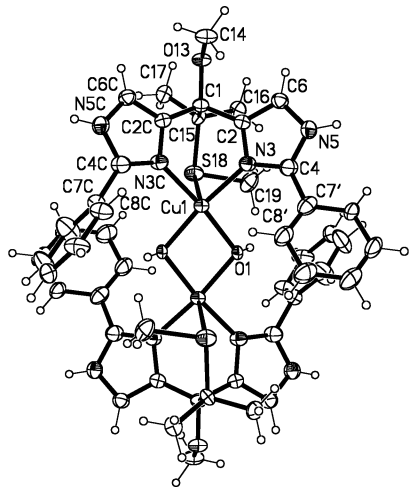

Figure 2. X-ray structure of **10**. Selected bond lengths (Å) and angles. Cu(1)−O(1) = 1.9208(16), Cu(1)−N(3) = 1.961(2), Cu(1)−S(18) = 2.7263(13), Cu(1)−Cu(1′) = 2.9985(12); O(1′)−Cu(1)−O(1) = 77.38(12), O(1)−Cu(1)−N(3) = 96.30(9), O(1)−Cu(1)−S(18) = 98.18(3), N(3)−Cu(1)−S(18) = 86.52(7), O(1)−Cu(1)−Cu(1′) = 38.69(6).

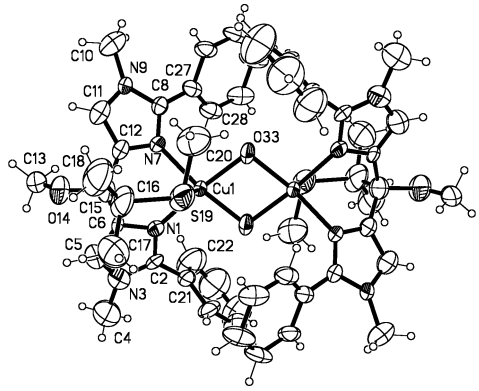

Figure 3. X-ray structure of **11**. Selected bond lengths (Å) and angles. Cu(1)−O(33) = 1.941(6), Cu(1)−N(1) = 1.984(8), Cu(1)−N(7) = 2.006(7), Cu(1)−S(19) = 2.757(3), Cu(1)−Cu(1′) = 3.028(2); O(33)−Cu(1)−N(1) = 174.9(3), O(33)−Cu(1)−N(7) = 96.5(3), N(1)−Cu(1)−N(7) = 88.4(3), O(33)−Cu(1)−S(19) = 92.81(19), N(1)−Cu(1)−S(19) = 86.4(3), N(7)−Cu(1)−S(19) = 84.7(3).

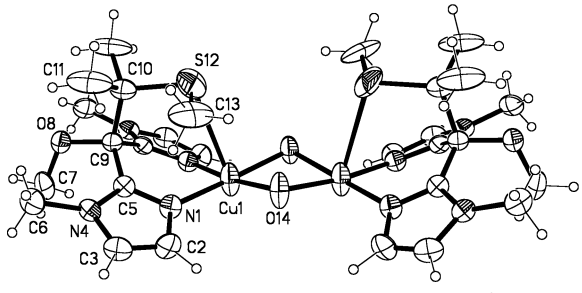

Figure 4. X-ray structure of **12**. Selected bond lengths (Å) and angles. Cu(1)−O(14) = 1.947(6), Cu(1)−N(1) = 1.944(5), Cu(1)−S(12) = 2.901(5); N(1)−Cu(1)−O(14) = 96.5(3), N(1)−Cu(1)−O(14′) = 95.9(3), N(1)−Cu(1)−S(12) = 81.83(18), O(14)−Cu(1)−S(12) = 94.3(9), O(14′)−Cu(1)−S12 = 114.610.

derivatives (*N*-Me (**11**), *N*-H (**10**)) are, as expected, isostructural and very similar to the previously characterized 2-tethered tripod derivative **2a**. The dinuclear dication in each has central inversion symmetry. Each Cu atom has a square pyramidal geometry with the base defined by the two imidazole nitrogens and the two bridging hydroxo oxygens and the apex by the thioether sulfur. Interestingly, the nonphenylated dinuclear dication of **12** displays C_2 symmetry with both Cu-centers again having square pyramidal geometry (Figure 4). The corresponding bond lengths (Å) and angles (deg) in the three complexes are very similar and unexceptional.

Computational Studies. To further probe the effects of substitutional variations of the tripodal ligands on the electronic character of the Cu(I)−L^+ complexes, we carried out semiempirical (PM3) and ab initio (DFT B3LYP) MO calculations. The faster PM3 method was best suited for the larger arylated complexes **17** (model for **1a**) and **18** (model for **8a**),[26] while the processing-intensive DFT method was utilized for the nonarylated derivatives, **13**−**16**, models for synthetic complexes **7a**, **8a**, and **9a**. In addition to molecular geometry, other properties calculated that are relevant to electronic character and reactivity include total energy, IR ν(CO), atomic charges, frontier MO energies, and distributions.

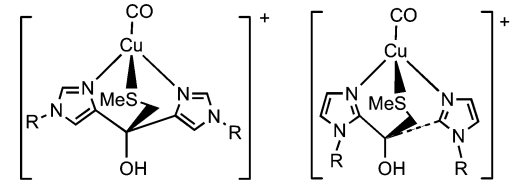

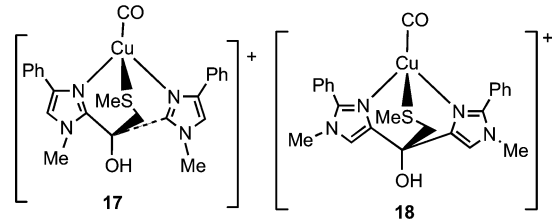

To evaluate the effects of the N-substituent (H vs Me) and the tethering position (2- vs 4-), DFT calculations were carried out on complexes **13**−**16**, following initial geometry optimization with the PM3 method. The resulting DFT-determined total energies, HOMO E and calculated ν(CO) are listed in Table 2. The calculated total energies of the pairs of isomeric 2- and 4-tethered tripod complexes (**13** and **15**, **14** and **16**), which should reflect thermodynamic stability (K_a), indicate that the 4-tethered complexes are more stable than the 2-substituted isomers by 5.6 and 11.9 kcal, respectively. The calculated HOMOs for these complexes have similar characteristics (Figure 5), being primarily S−Cu-imidazole π-bonding in character with a small Cu−C π-(back)bonding contribution but differing significantly in energy (the PM3-calculated HOMOs are qualitatively the same). The HOMOs for the 4-tethered complexes **13** and **14** were found at higher energy than the corresponding 2-tethered isomers **15** and **16** (by 3.7 and 3.7 kcal). A comparison of the *N*-Me versus *N*-H substituent effect on the HOMO energies, that is, **14** versus **13** and **16** versus **15**, shows a higher energy of 3.9 and 4.1 kcal/mol, respectively,

(26) Cundari, T. R.; Deng, J. *J. Chem. Inf. Comput. Sci.* **1999**, *39*, 376–381.

Table 2. Computational Data for [BIT)CuCO)]$^+$ Complexes

L/complex	E_T(H^c) or ΔH_f (kcal/mol)	νCu−CO (cm^{-1})	FMO energy (eV)	ESC^e Cu, N_1, N_3
[(4-BIT^{NH})CuCO]$^+$ (**13**)^a	−2796.073 H	2063 2071^d)	−8.99 (HOMO)	+0.31,−0.22, −0.09
[(4-BIT^{NMe})CuCO]$^+$ (**14**)^a	−2874.703 H	2059 (2066)^d	−8.81 (HOMO)	+0.30,−0.20, +0.51
[(2-BIT^{NH})CuCO]$^+$(**15**)^a	−2796.064 H	2071 (2070)^d	−9.15 (HOMO)	+0.32,−0.23, −0.26
[(2-BIT^{NMe})CuCO]$^+$(**16**)^a	−2874.684 H	2065 (2071)^d	>8.97 (HOMO)	+0.31,−0.20, +0.27
[(2-BIT$^{4\text{-}Ph,NMe}$)CuCO]$^+$ (**17**)^b	52.5 kcal	2166	−11.68(HOMO) −12.49 (HOMO−5)	−0.72, +0.25, −0.28
[(4-BIT$^{2\text{-}Ph,NMe}$)CuCO]$^+$ (**18**)^b	40.6 kcal	2156	−11.66 (HOMO)−12.37(HOMO−5)	−0.77, +0.37, +0.82

^{a} Calculated with DFT B3LYP. method. ^{b} Calculated with PM3 method. ^{c} ET = total electron energy, 1 H (Hartree) = 627.5 kcal. ^{d} Calculated with BP 6–31G** method. ^{e} Electrostatic charge.

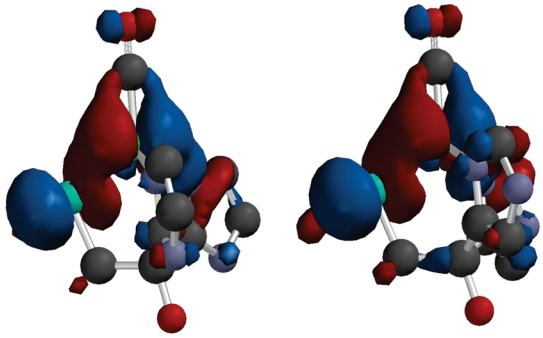

Figure 5. HOMOs for 2- and 4-tethered complexes **15** and **13,** respectively, (H's omitted).

for the Me derivatives. The computed Cu−CO IR frequencies for the four complexes varied modestly between 2059 and 2071 cm^{-1} (Table 2) and were inversely correlated with the respective HOMO energy, in the order **15** > **16** > **13** > **14**. Because the effectiveness of different DFT methods for accurately calculating transition metal–carbonyl vibrational frequencies (i.e., agreement with experiment) varies considerably,[27,28] we also employed the BP (6–31G**) method to calculate the vibrational spectra of **13**−**16** (Table 2). In this case, virtually no difference in the Cu−CO vibrational frequency among the complexes is calculated, varying only between 2066 and 2071 cm^{-1}, in agreement with the experimentally determined IR spectra of the synthetic complexes **1a**, **7a**, **8a**, and **9a**. Interestingly, although there is little difference in the calculated electrostatic charges at Cu (0.32, 0.31) or at the coordinated N (−0.23, −0.22) among the 4- vs the 2-tethered complexes **13** and **15**, the charges at the remote N (−0.25,−0.09) are quite different. Because the CV experiments were conducted on the acetonitrile adducts, parallel PM3 calculations on [(2-BIT^{NH})Cu(CH$_3$CN)]$^+$ and [(4-BIT^{NH})Cu(CH$_3$CN)]$^+$ revealed the same energy/HOMO effects operating as with the (BIT)Cu-COs, that is, the 4-tethered complex is of lower total energy (−2.5 kcal) and has a higher energy HOMO (+3.9 kcal).

The electronic character of the phenylated complexes was probed by semiempirical PM3 level calculations. Because the structures of the newly prepared [(BIT)CuL]$^+$ complexes have not been determined crystallographically, the effectiveness of the PM3 method to determine molecular geometry for this class of complexes was first evaluated from calculations on the X-rayed [(2-BIT^{Ph2,NMe,OH})Cu(CO)]PF$_6$ (**1a**). The overall trigonal pyramidal geometry of **1a** was reasonably reproduced as is generally found with the PM3 method.[23b,26] The calculated bond lengths and angles were generally within 5% of the experimental, but significant differences (10–12%) were found in a few metrics, notably the Cu−S distances and the C−Cu−N angles. A selection of the bond lengths and angles around the Cu center from the X-ray structure (*and calculated*) of **1a** follows: Cu−C = 1.811(2) (*1.905*), Cu−N(1) = 2.0005(19) (*1.916*), Cu−N(2) = 2.0259(17) (*1.916*), Cu−S = 2.4392(7) (*2.178*), C−O = 1.123(2) (*1.156*); C−Cu−N(2) = 122.90(9) (*119.1*), C−Cu−N(1) = 132.84(10) (*119.5*), C−Cu−S = 118.81(9) (*120.7*), N−Cu−N = 90.67(7) (*94.1*), N(2)−Cu−S = 93.37(6) (*101.6*), N(1)−Cu−S = 87.33(5) (*96.4*), Cu−C−O = 177.4(2) (*179.2*).

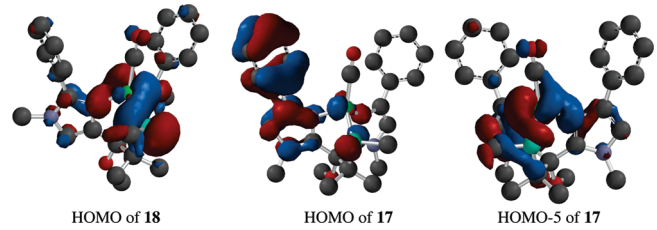

Figure 6. HOMOs of **18** and **17** and the HOMO−5 of **17**.

To assess the effects of the tripodal 2/4-tethering and aryl group positions the isomeric complexes **17** and **18** were compared (Table 2). As was the case with the DFT results on the nonarylated derivatives, the 4-tethered complex **18** is calculated to be significantly more stable (∼12 kcal) than the 2-tethered **17**. Once again, the 4-tethered **18** is calculated to have a modestly lower (∼10 cm^{-1}) Cu−CO vibrational frequency, but in contrast to the results on the nonarylated complexes, little difference in the HOMO energies (0.02 eV) is calculated. Inspection of the HOMO distribution in the arylated complexes (Figure 6) found it to be dependent on the tripodal tethering position and, for the 2-tethered derivative **17**, to be quite different from that of the nonaryl derivatives. The HOMO of 4-tethered **18**, like the nonphenyl derivatives **13**−**16**, is primarily S−Cu π-bonding in character with a small Cu−CO backbonding component. In contrast, the HOMO of the 2-tethered **17** (Figure 6), is largely localized on the aryl groups and the imidazoles with modest Cu, S contributions. At lower energy, HOMO−5 of **17** is similar in character to the HOMO of the nonarylated derivatives, with S−Cu−imid π-bonding and a small Cu−CO backbonding interaction. Comparing the relative energies of HOMO−5 and the computed Cu−CO vibrational frequencies

(27) Bolsjakov, V. I.; Rossikhin, V. V.; Voronkov, E. O.; Okovytyy, S. I.; Leszczynski, J. *J. Comput. Chem.* **2007**, *28*, 778–782.
(28) Feng, X.-J.; Gu, J.-D.; Xie, Y.-M.; King, B. R.; Schaefer III, H. F. *J. Chem. Theory Comput.* **2007**, *3*, 1580–1587.

for the 4- versus 2-tethered complexes (Table 2), we find, as with the nonarylated complexes, that the 4-tethered derivative **18** has a higher energy partially backbonding FMO and corresponding lower-energy calculated Cu−CO vibration. Because the oxygenation reactions of **1a′** and **7b′**−**9b′** are likely to involve initial association of O_2 with a coordinatively unsaturated $[(BIT)Cu]^+$ species, the relative stability and FMO energies of the isomeric 2- and 4-tethered complexes are potentially relevant to understanding their relative reactivity. A PM3-level comparison of the nonphenylated $[(2\text{-}BIT^{NH,OH})Cu]^+$ (E_{tot} = 32.28 kcal, E_{HOMO}= −11.87 eV) and $[(4\text{-}BIT^{NH,OH})Cu]^+$ (29.77 kcal, −11.70 eV) found, as with the $[(BIT)Cu(L)]^+$ derivatives, that the 4-tethered complex was lower in energy than the 2-isomer and had a higher-energy HOMO.

Discussion

We have prepared a new set of tripodal N_2S-(BIT) ligands and derived Cu^I complexes that possess the biologically relevant imidazole/thioether donor set of the Cu_M site of the Cu-hydroxylase enzymes. Our objective was to ascertain the influence of ligand-derived steric and electronic effects on the electronic character and oxidative reactivity of the resulting Cu(I) complexes. The ligands differ in the steric/electronic character and position of the imidazole substituents, specifically the C-2/4-position of the tripodal tether, the presence (absence) of *C*-phenyl and of *N*-Me versus *N*-H substituents. The more histidine-like 4-tethered ligands were efficiently prepared using a regioselective metalation/protection sequence that provides access to the imidazole *N*-Me and *N*-H and the tripodal *C*-OH and *C*-OMe derivatives selectively. Electronically speaking, one would expect *N*- or *C*-alkyl substituents on the imidazole units to increase their basicity (and σ-donor ability). This is supported by the determined pK_a values of alkyl-imidazoles,[29] reported K_{assoc} of some imidazole-metal ion complexes,[30] and the Breslow study showing that 4-tethered $(imid)_3COH$ form more stable complexes with Zn(II) and Cu(II).[24] While aryl- for H-substitution will clearly increase steric bulk in the vicinity of the Cu−L center, the electronic impact is less certain, with a balance between electron-donating inductive/field effects and electron-releasing resonance effect.[31]

Each of the complexes readily forms an isolable CO adduct. Several studies of N_3-Cu-CO derivatives have shown a correlation between total complex charge and L-donor/acceptor properties with ν(CO), with neutral complexes and those with more electron-donating ligands, showing lower ν(CO), consistent with increased backbonding.[23] Somewhat unexpectedly, therefore, we found that the Cu−CO ν(CO) hardly varied among the complexes **1a** and **7a**−**9a**. Although this could be taken to indicate there was little electronic difference among these complexes, the CV, dioxygen reactivity, and MO calculations indicate otherwise.

The electrochemical $E_{1/2}$ oxidation potential reflects the energy needed for electron removal/addition at the electrode surface/solution interface in converting $[(BIT)Cu^IL]^+$ to $[(BIT)Cu^{II}L]^{2+}$ and back. The quasi-reversible nature of the CV waves for **1a′**, **7b′**, and **8b′** (L = CH_3CN) may be the result of significant structural reorganization of the $[(BIT)Cu^{II}L]^{2+}$ species occurring upon oxidation, from chemical instability of the $[(BIT)Cu^{II}L]^{2+}$or from slow electron-transfer kinetics on the electrode surface. Since true $E_{1/2}$ values could not be determined, the potentials corresponding to Cu^I/Cu^{II} oxidation peaks (E_{pa}) relative to $E_{1/2}$ for ferrocene were used to enable semiquantitative comparisons of the ease of $[(BIT)Cu^IL]^+$ oxidation among this set of complexes.[16,25] The order of the E_{pa} values, **7b′** > **1a′** > **8b′** > **9b′**, parallels the anticipated electronic effects of the various substituents. Thus, complex **8b′**, having the electron-releasing *N*-Me group, is easier to oxidize than the *N*-H relative **7b′**. A comparison of the 2-tethered, *N*-Me complexes **1a′** and **9b′**, with and without Ph-groups, shows the latter to be more easily oxidized than the former, consistent with a net electron-withdrawing effect of the Ph-group. The phenylated 4-tethered tripod complex **8b′** is more easily oxidized than the 2-tethered relative (**1a′**). This could be ascribed in part to the electronic differences derived from the tethering position but also probably reflects the lesser net electron withdrawal from two phenyl groups of **8b′** versus the four phenyls of **1a′**. It is not possible to quantitatively compare the oxidation potentials of the present $[(BIT)CuL]^+$ complexes with the Karlin tridentate $[N_2S-Cu-L]^+$ compounds that have a pyridine-alkyl amine-thioether donor set since the latter are reported to undergo irreversible oxidation at about +400–500 mV vs/$Fc^{(0,+)}$.[16]

The differences in reactivity of **1a′** and **7b′**−**9b′** toward oxygen, signaled by the Cu^I/Cu^{II} color change, are quite remarkable, ranging from minutes at −50 to −70 °C for **8b′** and **9b′** to hours at room temperature for **7b′** and **1a′**. These qualitative reactivities reflect the composite rate of reaction over several steps, presumably including $[(BIT)Cu\text{-}CH_3CN)]^+$ dissociation, O_2 association with $[(BIT)Cu]^+$ to form $[(BIT)Cu-O_2]^+$, and subsequent steps (in unknown order), involving binuclear complex formation and H-atom abstraction, to form the copper hydroxo-dimer products **10**−**12**. Although we have no information yet on the kinetics or the detailed mechanism of these oxygenations, the absence of obvious transient colored species that would signal long-lived intermediates, suggests that an early step, for example, $[(BIT)Cu(CH_3CN)]^+$ dissociation or $[(BIT)Cu]^+ + O_2$ association, is likely rate-limiting. If the latter is the case, one would expect that the more electron-rich $[(BIT)Cu]^+$ species would be more reactive (and form a more stable complex) with the electrophilic dioxygen.[24b] Likewise, the same factor is expected to facilitate electrochemical oxidation of the $[(BIT)Cu-L]^+$ complexes since both processes fundamentally involve partial/complete electron removal from the Cu(I). Indeed, a correlation between redox potentials and dioxygen reactivity has been noted in other studies of Cu(I)

(29) (a) El Ghomari, M. J.; Mokhlisse, R.; Laurence, C.; Le Questel, J.-Y.; Berthelot, M. *J. Phys. Org. Chem.* **1997**, *10*, 669–674. (b) Ramsey, B. G. *J. Org. Chem.* **1979**, *44*, 2093–2097.
(30) Paiva, A. C. M.; Juliano, L.; Boschcov, P. *J. Am. Chem. Soc.* **1976**, *98*, 7645–7648.
(31) March, J. *Advanced Organic Chemistry*, 4th ed; Wiley: New York, 1992; pp. 280–284.

complexes.[32] However, unless Cu−O_2 association involves initial electron transfer,[33] followed by recombination to form the Cu−O_2 complex, the electronic details of the two processes would not be identical and a perfect correlation would not be expected. Aside from the electronic effects underlying the redox and oxygenation reactivity differences among **1a′** and **7b′**−**9b′**, the generally lower oxygenation reactivity of the phenylated complexes vis a vis the nonphenylated ones, may in part result from steric inhibition, kinetic or thermodynamic, to oxygen association (and subsequent dinuclear complex formation).

The oxygenation results of the [(BIT)CuL]$^+$ complexes can be compared and contrasted with Karlin's non-imidazole N_2S−Cu complexes[16] and other N_3−Cu complexes. Two of the former were found to be unreactive with O_2 between −40 and −80 °C, and their oxygenation at room temperature over minutes/hour afforded complexes in which thioether *S*-oxidation had occurred, a pathway not observed with the BIT−Cu complexes. The [(BIT)CuL]$^+$ compounds **8b′** and **9b′** thus appear to be the most reactive toward dioxygen of the N_2S−Cu complexes prepared to date and are comparable to several of the reported N_2− and N_3−Cu model systems.[12,15,19,20] The fundamental question raised here is what electronic parameters control these two related reactions, ionization and oxygenation, and the IR Cu−CO vibrational frequency?

The computational results on the various [(BIT)Cu−CO]$^+$ complexes aid to some extent in clarifying the importance of various electronic factors that determine the experimental measurables of ν(Cu−CO), redox potential and oxygenation reactivity. Before addressing these points, however, we note the consistent calculational finding that Cu^I complexes of the 4-tethered (histidine-like) N_2S-ligands are of lower energy (i.e., are more stable) than the 2-tethered derivatives; the calculated energy difference ranges from 5.7 kcal from DFT on **13**/**15** to 11.9 kcal by PM3 on the phenylated **17**/**18**. Although experimental data supporting this result for the [(BIT)Cu^{I}L]$^+$ complexes are not yet available, the greater formation constants of the 4- versus 2-tethered (imid)$_3$COH ligands with some M^{II} ions was established by Breslow et al.[21] A simple electronic explanation for this effect is not obvious because the pK_a values of alkyl-substituted imidazoles show the 2-substituted derivatives to be more basic (∼0.5 pK_a units) than the 4-substituted ones.[29] In contrast, the Breslow study showed the greater basicity of the 4-tethered over the 2-tethered tris(imidazolyl) ligands, ascribing it to greater (stabilizing) charge separation in the protonated (and coordinated) 4-tethered derivatives. Although there is little difference in the calculated electrostatic charges of the 2- versus 4-tethered complexes at copper or the coordinated nitrogen, the calculated charges at the remote nitrogen are quite different, consistent with the Breslow explanation. However, the total energy/stability of each complex is the result of the sum of all the electron energies, which include multiple electronic interactions, and hence, the origin of the greater stability of the 4-tethered ligand complexes is not readily explained by a single dominant interaction.

The electrochemical oxidation potential for the [(BIT)Cu−L]$^+$ complexes is a measure of the free energy change accompanying the removal of a valence electron from [(BIT)Cu^{I}L]$^+$ to produce [(BIT)Cu^{II}L]$^{2+}$ in solution. Accurate calculations of $E_{1/2}$ would thus require the energies of both initial and final copper-containing species in solution. Because of uncertainties associated with obtaining accurate energies of the paramagnetic N_2S-Cu^{II} species, including solvent effects and electrode surface overpotentials, and the nonideal electrochemical behavior for the present complexes, rigorous calculations of the electrochemical oxidation potentials were judged impractical.[34] To the first approximation, however, trends in E_{pa} could be estimated from the E(HOMO)[35] of the [(BIT)Cu−L]$^+$ complexes because this approximates the energy of the electron to be removed. Indeed, the calculated HOMO energies among the various [(BIT)Cu(CO)]$^+$ complexes parallel their ease of electrochemical oxidation. The imidazole-substitutional effects on the [(BIT)CuL]$^+$ complexes suggested by the computational studies apparently hold for both the carbonyl and the acetonitrile complexes since PM3 calculations on [(2-BIT)Cu(CH$_3$CN)]$^+$ and [(4-BIT)Cu(CH$_3$CN)]$^+$ found the same total energy/HOMO effects as the [(BIT)CuCO]$^+$, that is, the 4-tethered complex is of lower energy and has a higher-energy HOMO. Comparison of the HOMO energies of the phenylated and nonphenylated complexes is not possible because of the use of different computational methods.

A thorough computational analysis of [(BIT)Cu(O_2)]$^+$ reactivity should consider the energy profile of the complete stepwise conversion of [(BIT)Cu(L)]$^+$ + O_2 to products, especially the rate-limiting step. Given the present lack of mechanistic information on these reactions, such an analysis is beyond the scope of the current study but is the subject of an ongoing investigation. However, if [(BIT)Cu(L)]$^+$ + O_2 association or electron transfer is rate-limiting (consistent with the apparent absence of long-lived intermediates), then the energy of the HOMO of sixteen electron [(BIT)Cu]$^+$ (for O_2 association) or eighteen electron [(BIT)Cu(L)]$^+$ (for ET) should be an important factor in determining reactivity, that is, the complexes with a higher *E*(HOMO) should be more effective (stabilizing) backbonders to O_2 in [(BIT)Cu(O_2)]$^+$ and also be more easily oxidized. For the [(BIT)Cu(L)]$^+$ complexes, the HOMO energies of the various derivatives (Table 2) do parallel their reactivity toward dioxygen (Table 1), with the 4-tethered, *N*-methylated or nonphenylated derivatives having the higher HOMO energies and being more readily oxygenated. This appears to be the case for

(32) (a) Baldridge, K. K.; Donovan-Merkert, B. T.; O'Connor, J. M.; Lee, L. I.; Closson, A.; Fandrick, D.; Tran, T.; Bunker, K. D.; Fouzi, M.; Gantzel, P. *Org. Biomol. Chem.* **2003**, *1*, 763–766. (b) Klinman, J. P. *J. Biol. Chem.* **2006**, *281*, 3013–3016.

(33) Kamachi, T.; Kihara, N.; Shiota, Y.; Yoshizawa, K. *Inorg. Chem.* **2005**, *44*, 4226–4236.

(34) (a) Riahi, S.; Moghaddam, A. B.; Ganjali, M. R.; Norouzi, P.; Latifi, M. *THEOCHEM* **2007**, *807*, 137–145. (b) Reynolds, C. A. *J. Am. Chem. Soc.* **1990**, *112*, 7545–7551.

(35) Ue, M.; Murakami, A.; Nakamura, S. *J. Electrochem. Soc.* **2002**, *149*, A1572–A1577.

the electronically unsaturated $[(BIT)Cu]^+$ complexes as well because a PM3 calculational comparison of the sixteen electron $[(2\text{-}BIT^{NH})Cu]^+$ and $[(4\text{-}BIT^{NH})Cu]^+$ shows that the 4-tethered form is more stable but has the higher-energy HOMO. A more rigorous analysis will include computations (and structures, stabilities) on the $[(BIT)Cu(O_2)]^+$ complexes that are in progress. The above computational analysis ignores steric effects, which are likely to be minimal in comparing the *N*-Me to the *N*-H derivatives and the 2- versus 4-tethered tripodal ligands. However, complexes of the phenylated ligands (e.g., **1**, **7**, **8**) could be of attenuated oxygenation reactivity relative to the nonarylated derivative **9** because of a combination of stabilizing electronic effects and kinetically retarding steric effects to the approach of O_2.

Finally, we have found that the calculational methods employed vary in their effectiveness of reproducing the experimentally observed invariance of the Cu−CO vibrational frequencies among **1a** and **7a–9a**. The PM3 method calculates $\nu_{(Cu\text{-}CO)}$ values substantially higher (60–70 cm^{-1}) than experimentally observed and predicts a significant effect (10 cm^{-1}) of the position of the tripodal imidazole alkyl tether. The DFT methods, B3LYP and BP applied to **13–16**, fare better in reproducing the experimental $\nu_{(Cu\text{-}CO)}$ values for $[(BIT)Cu(CO)]^+$ (**1a**, **7a–9a**), both with respect to magnitude (underestimating by 25–30 cm^{-1}) and to the substituent effects. The B3LYP method calculates a small effect (∼5 cm^{-1}) of *N*-Me versus *N*-H and 4-BIT versus 2-BIT substitution, following a trend expected from simple inductive effects, but only over a 12 cm^{-1} range for **13–16**. The BP DFT method, found to more accurately calculate $\nu_{(M\text{-}CO)}$ values of binary metal–carbonyls,[27,28] predicts virtually no difference in $\nu_{(Cu\text{-}CO)}$ among **13–16** (total range = 5 cm^{-1}) and no systematic substituent effects, in accord with the experimental IR data for **1a**, **7a–9a**. Although chemists often consider the M−CO frequency as being largely determined by the balance between two interactions, the CO-to-M σ-donation and the M-to-CO π-backbonding, extensive MO mixing and multiple orbital contributions to the M−CO interaction may complicate quantitative predictions. The pitfalls of the two (or one) interaction explanation for IR Cu−CO frequencies in the present systems is also complicated by the changing character (atomic distribution) of the FMOs between the phenylated versus nonphenylated complexes and the differences in the FMO energies among the isomeric 4- versus 2-tethered derivatives. Although the E_{HOMO} for the 4-tethered complexes was consistently found at higher energy than for the 2-tethered compounds with all the computational methods, the partially "backbonding" Cu−CO orbital is the HOMO for the nonphenylated complexes (**13–16**) and for the 4-tethered phenylated **18**, but it is "buried" as HOMO−5 in the 2-tethered Ph-complex **17**. Regardless of the electronic reason for the nonvariability of the experimental Cu−CO absorption in the series, our experimental and calculational findings caution against using the M−CO IR vibrational frequency as a reliable indicator of electronic character (e.g., metal electron density, single orbital backbonding).

Conclusions

New bis(imidazole)thioether (N_2S)−copper complexes that incorporate the ligand set of the Cu_M site of the copper hydroxylase enzymes have been prepared and characterized. This investigation has shown that imidazole-based substituent variations on the BIT ligands can have important effects on the oxygenation and electrochemical oxidation of corresponding $[(BIT)Cu-L]^+$ complexes. In general, 4-tethering, analogous to that found in histidine-coordinated metalloenzymes, and N-methylation increase electrochemical oxidation and oxygenation reactivity, while C-arylation decreases reactivity. The effects of imidazole alkyl substitution on the stability and reactivity of the (BIT)Cu(I) complexes examined herein will enable us to more accurately mimic the active site of copper redox enzymes. On the other hand, within this set of complexes the Cu−CO IR vibrational frequency is a poor predictor of oxidative reactivity. Finally, in spite of strong evidence that dioxygen coordination/activation occurs at the N_2S-Cu_M site of the hydroxylase enzymes, there has been a perception from some model studies that N_2S−Cu complexes are inherently less reactive toward dioxygen than N_3-Cu species. Our findings, which include rapid oxygenation reactions of two $[(BIT)CuL]^+$ complexes at low temperature, indicate that this is not necessarily so. Further reactivity and mechanistic studies of these systems and the development of still more accurate structural and functional mimics of the copper hydroxylase enzymes are continuing.

Experimental Section

Materials and Methods. All operations were carried out under nitrogen or argon by means of standard Schlenk and vacuum-line techniques. CH_2Cl_2 was dried over CaH_2 and distilled under N_2; THF was dried over Na using benzophenone as indicator and distilled under N_2. Glassware was oven-dried at 150 °C overnight. A Vacuum Atmospheres drybox was used in the handling of air-sensitive solids. IR spectra were recorded in either CH_2Cl_2 solution or in KBr pellets with a Perkin-Elmer 283-B infrared spectrophotometer (resolution 4 cm^{-1}). The ^1H and ^{13}C NMR spectra were recorded on a Varian Mercury-300 spectrometer. Mass spectra were obtained on a Finnigan TSQ 700 ESI instrument in methanol or acetonitrile solution. Elemental analyses were performed by Midwest Microlab, LLC. Electrochemical measurements were performed in freshly distilled CH_2Cl_2 with a BAS CV-50W instrument. A three-electrode cell was used (Pt working and auxiliary electrodes, Ag/AgCl reference electrode). Potentials were recorded versus ferrocene. Scans were run at 50–400 mV/s under a nitrogen atmosphere. The solutions were ca. 1.0 mM in analyte in 10 mL of ca. 0.1 M NBu_4PF_6 as the supporting electrolyte. Nitrogen gas was bubbled through the solution for about 10 min before each set of measurements and was passed continuously over the surface of the solution during the measurements. *N*-Ethoxymethyl-2-phenylimidazole[22] and compounds **1a**, **1a′**[19] were prepared according to reported procedures. $[Cu(CH_3CN)_4]PF_6$ was obtained commercially.

1,1-Bis(*N*-ethoxymethyl-2-phenyl-5-imidazolyl)-2-methyl-2-methylthio-propanol (3a, $BIT^{2\text{-}Ph,NEOM,OH}$). To a solution of *N*-ethoxymethyl-2-phenylimidazole (2.42 g, 12.0 mmol) in 30 mL of dry THF under N_2 cooled to −78 °C was added *n*-BuLi dropwise (6.30 mL in hexane, 10.8 mmol). The mixture was stirred at this temperature for 2 h to give a dark green solution. After dropwise

addition of dry ethyl 2-methyl-2-methylthiopropinate (0.79 mL, 5.4 mmol), the mixture was allowed to warm to room temperature overnight to give an orange solution. The reaction was quenched with 80 mL of water, extracted with diethyl ether, and the organic phase was dried over $MgSO_4$. Flash column chromatography (silica) using petroleum ether/ethyl acetate (1:1) as eluant gave 1.60 g (57%) of the alcohol **3a** as a white solid. ^{1}H NMR (300 MHz, CD_2Cl_2): δ 1.06(t, J = 7 Hz, 6H), 1.61(s, 6H), 1.99(s, 3H), 3.27(m, 4H), 5.11(d, J = 8 Hz, 2H), 5.30(d, J = 8 Hz, 3H, CH_2 + COH), 7.31(s, 2H), 7.43–7.47(m, 6H), 7.63–7.66(m, 4H). ^{13}C NMR (75 MHz, CD_2Cl_2): δ 150.9, 133.5, 131.3, 131.2, 129.8, 129.6, 128.9, 80.1, 74.6, 63.9, 56.7, 26.0, 15.0, 13.4. HRMS (ESI) m/z 521.2574 (M + 1); calcd for $C_{29}H_{37}N_4O_3S$ 521.2586. IR (KBr; cm^{-1}): 2973, 2927, 2857, 1652, 1559, 1508, 1458, 1090. Anal. Calcd for $C_{29}H_{36}N_4O_3S$: C, 66.89; H, 6.97; N, 10.76. Found: C, 66.71; H, 7.03; N, 10.58.

1-Methoxy-2-methyl-1,1-bis-(*N*-ethoxymethyl-2-phenyl-5-imidazolyl)-2-methylthiopropane (3b, BIT$^{2\text{-Ph,NEOM,OMe}}$). Sodium hydride (170 mg, 60% mineral oil suspension, 4.30 mmol) was suspended in dry THF (20 mL) under N_2. Compound **3a** (1.80 g, 3.46 mmol) dissolved in dry THF (20 mL) was added dropwise to the NaH suspension over 2 min, and the resulting mixture was stirred for 2 h at room temperature until no bubbles appeared. Methyl iodide (260 μL, 4.30 mmol, 1.20 equiv) was added dropwise, and then the reaction mixture was stirred for 24 h. Then the reaction was quenched with 40 mL of deionized water and extracted twice with 25 mL portions of ether, and the organic phase was dried over $MgSO_4$. Rotary evaporation of the ether gave 0.78 g of **3b** as a light yellow solid (42%) which was used in the next step without further purification.

1,1-Bis(*N*-*H*-2-phenyl-4(5)-imidazolyl)-2-methyl-2-methylthio-propanol (4a, 4-BIT$^{2\text{-Ph,NH,OH}}$). Compound **3a** (100 mg, 0.19 mmol) was dissolved in the mixture of 5 mL of methanol and 10 mL of a 3 M HCl aqueous solution. The resultant mixture was refluxed under N_2 for 18 h to give a colorless solution. After it was cooled, the reaction mixture was quenched with 40 mL of brine, neutralized with concentrated ammonium hydroxide, and extracted twice with 30 mL portions of CH_2Cl_2, and the organic phase was dried over $MgSO_4$. Rotary evaporation of CH_2Cl_2 gave 70 mg of **4a** as a light yellow solid (90%). ^{1}H NMR (300 MHz, CD_2Cl_2): δ 1.44(s, 6H), 1.80(s, 3H), 3.42(s, 1H), 7.23(s, 2H), 7.35–7.49(m, 6H), 7.84–7.86(m, 4H). ^{13}C NMR (75 MHz, CD_2Cl_2): δ 145.4, 130.8, 129.4, 129.1, 125.4, 76.9, 60.2, 24.9, 13.3. HRMS (ESI) m/z 405.1740 (M+1); calcd for $C_{23}H_{25}N_4OS$ 405.1749. IR (KBr; cm^{-1}): 3399, 2985, 2828, 1700, 1652, 1560, 1459, 1260, 1083, 694. Anal. Calcd for $C_{23}H_{24}N_4OS$: C, 68.29; H, 5.98; N, 13.85. Found: C, 68.83; H, 6.29; N, 13.75.

1-Methoxy-2-methyl-1,1-bis-(*N*-*H*-2-phenyl-4(5)-imidazolyl)-2-methylthiopropane (4b, 4-BIT$^{2\text{-Ph,NH,OMe}}$). Compound **3b** (210 mg, 0.39 mmol) was dissolved in a mixture of 20 mL of freshly dry methanol and 4 mL of trifluoroacetic acid (TFA). The resultant mixture was refluxed under N_2 for 12 h to give a colorless solution. After it was cooled, the reaction mixture was quenched with 40 mL of brine, neutralized with concentrated ammonium hydroxide, and extracted twice with 30 mL portions of CH_2Cl_2, and the organic phase was dried over $MgSO_4$. Flash column chromatography (silica) using petroleum ether:ethyl acetate (1:1) as eluant gave 80 mg (49%) of **4b** as a white solid. ^{1}H NMR (300 MHz, CD_3OD): δ 1.31(s, 6H), 1.93(s, 6H), 3.22(s, 3H), 7.19(s, 2H), 7.38–7.50(m, 6H), 7.84–7.92(m, 4H). ^{13}C NMR (75 MHz, CD_3OD): δ 129.1, 128.7, 125.2, 85.0, 52.8, 52.4, 24.4, 12.4. HRMS (ESI) m/z 419.1823 (M + 1); calcd for $C_{24}H_{27}N_4OS$ 419.1906. IR (KBr; cm^{-1}): 3071, 2985, 2927, 2828, 1700, 1652, 1560, 1509, 1459, 1260, 1228, 1137, 1083, 694. Anal. Calcd for $C_{24}H_{26}N_4OS$: C, 68.87; H, 6.26; N, 13.39. Found: C, 67.98; H, 6.20; N, 13.10.

1,1-Bis-(*N*-methyl-2-phenyl-4-imidazolyl)-2-methyl-2-methylthio-propanol (5a, 4-BIT$^{2\text{-Ph,NMe,OH}}$). Sodium hydride (55 mg, 60% mineral oil suspension, 1.3 mmol) was suspended in dry THF (15 mL) under N_2. A solution of **4a** (160 mg, 0.40 mmol) dissolved in dry THF (15 mL) was added dropwise to the NaH suspension over 2 min, and the resulting mixture was stirred for 2 h at room temperature until no bubbles appeared. Methyl iodide (82 μL, 1.3 mmol) was added dropwise, and then the reaction mixture was stirred for 24 h to give a yellow solution. The reaction was quenched with 4 mL of methanol. Rotary evaporation of the solvent and then flash column chromatography (silica) of the residue using ethyl acetate as eluant gave 70 mg (41%) of **5a** as a light yellow solid. ^{1}H NMR (300 MHz, CD_2Cl_2): δ 1.48(s, 6H), 1.84(s, 3H), 3.71(s, 6H), 5.17(s, 1H), 7.27(s, 2H), 7.40–7.48(m, 6H), 7.63–7.66(m, 4H). This isomer was confirmed by 1D-NOESY, which showed an interaction between *N*-Me and imidazole vinyl H and an interaction between *N*-Me and *C*-Ph when the *N*-Me was irradiated. ^{13}C NMR (75 MHz, CD_2Cl_2): δ 145.6, 144.4, 131.5, 129.0, 128.9, 128.8, 121.3, 77.8, 60.8, 35.0, 25.0, 13.1. HRMS (ESI) m/z 433.2104 (M + 1); calcd for $C_{25}H_{29}N_4OS$ 433.2062. IR (KBr; cm^{-1}): 3149, 3063, 2970, 2926, 2861, 1473, 1388, 1296, 1137, 1075, 775, 698. Anal. Calcd for $C_{25}H_{28}N_4OS$: C, 69.41; H, 6.52; N, 12.95. Found: C, 69.31; H, 6.36; N, 12.64.

1-Methoxy-2-methyl-1,1-bis-(*N*-methyl-2-phenyl-4-imidazolyl)-2-methylthiopropane (5b, 4-BIT$^{2\text{-Ph,NMe,OMe}}$). Sodium hydride (20 mg, 60% mineral oil suspension, 0.50 mmol) was suspended in dry THF (10 mL) under N_2. Compound **5a** (140 mg, 0.32 mmol) dissolved in dry THF (10 mL) was added dropwise to the NaH suspension over 2 min, and the resulting mixture was stirred for 2 h at room temperature until no bubbles appeared. Methyl iodide (30 μL, 0.38 mmol) was added dropwise, and then the mixture was stirred for 24 h to give a yellow solution. The reaction was quenched with 40 mL of brine and extracted twice with 20 mL portions of CH_2Cl_2, and the organic phase was dried over $MgSO_4$. Rotary evaporation of the solvent and then flash column chromatography (silica) of the residue using ethyl acetate as eluant gave 100 mg (70%) of **5b** as a white solid. ^{1}H NMR (300 MHz, CD_2Cl_2): δ 1.48(s, 6H), 1.81(s, 3H), 3.22(s, 3H), 3.76(s, 6H), 7.40–7.48(m, 8H), 7.60–7.70(m, 4H). ^{13}C NMR (75 MHz, CD_2Cl_2): δ 146.1, 141.1, 131.9, 129.1, 129.0, 128.7, 125.1, 85.5, 64.1, 35.1, 25.5, 13.1. HRMS (ESI) m/z 447.2242 (M + 1); calcd for $C_{26}H_{31}N_4OS$ 447.2219. IR (KBr; cm^{-1}): 2972, 2930, 2861, 14753, 1076, 942, 775, 703. Anal. Calcd for $C_{26}H_{30}N_4OS$: C, 69.92; H, 6.77; N, 12.54. Found: C, 69.45; H, 6.82; N, 12.66.

1,1-Bis-(*N*-methyl-2-imidazolyl)-2-methyl-2-methylthio-propanol (6a, 2-BIT$^{\text{NMe,OH}}$). To a solution of *N*-methylimidazole (1.03 g, 12.5 mmol) in 20 mL dry THF under N_2 cooled to –78 °C was added *n*-BuLi dropwise (8.90 mL in hexane, 12.5 mmol). The mixture was stirred at this temperature for 2 h to give a light yellow solution. After addition of dry ethyl 2-methyl-2-methylthiopropinate dropwise (0.93 mL, 6.25 mmol), the mixture was allowed to warm to room temperature overnight to give an orange solution. The mixture was quenched with 80 mL of water and extracted with CH_2Cl_2, and the organic phase was dried over $MgSO_4$. Rotary evaporation of the solvent gave 1.0 g of **6a** as colorless crystals (57%). ^{1}H NMR (300 MHz, $CDCl_3$): δ 1.71(s, 6H), 1.73(s, 3H), 3.12(s, 6H), 5.30(s, 1H), 6.76(d, J = 1.2 Hz, 2H), 6.98(d, J = 1.2 Hz, 2H). ^{13}C NMR (75 MHz, $CDCl_3$): δ 146.7, 126.0, 123.5, 80.9, 54.7, 34.3, 25.4, 13.5. HRMS (ESI) m/z 281.1421 (M + 1); calcd for $C_{13}H_{21}N_4OS$ 281.1436. IR (KBr; cm^{-1}): 3233, 2998, 2967, 2931,

Table 3. X-ray Diffraction Collection Data for **10**−**12**

	10	**11**	12
empirical formula	$(C_{48}H_{52}Cu_2N_8O_4S_2)(PF_6)_2$	$(C_{52}H_{60}Cu_2N_8O_4S_2)(PF_6)_2(H_2O)_{0.5}$	$(C_{28}H_{44}Cu_2N_8O_4S_2)(PF_6)_2$
fw	1288.13	1351.23	1037.85
cryst syst	monoclinic	monoclinic	orthorhombic
space group	*C*2/*m*	*C*2/*c*	*Pmmn*
unit cell dimensions	$a = 20.615(6)$ Å	$a = 24.906(12)$ Å	$a = 17.010(8)$ Å
	$b = 13.416(4)$ Å	$b = 14.336(6)$ Å	$b = 17.712$ Å
	$c = 11.190(3)$ Å	$c = 17.529(8)$ Å	$c = 6.801(4)$ Å
	$\alpha = 90°$	$\alpha = 90°$	$\alpha = 90°$
	$\beta = 118.276(8)°$	$\beta = 100.240(8)°$	$\beta = 90°$
	$\gamma = 90°$	$\gamma = 90°$	$\gamma = 90°$
vol	2725.5(14) Å^3	6159(5). Å^3	2049.0(19) Å^3
Z, *Z*′	2, 0.25	4, 0.5	2, 0.25
density	1.570 Mg/m^3	1.457 Mg/m^3	1.682 Mg/m^3
wavelength	0.71073 Å	0.71073 Å	0.71073 Å
temp	100(2) K	100(2) K	100(2) K
F(000)	1316	2772	1056
abs coeff	1.008 mm^{-1}	0.896 mm^{-1}	1.318 mm^{-1}
abs correction	semiempirical equiv	semiempirical equiv	semiempirical equiv
max., min. transm	0.974, 0.631	0.966, 0.797	0.939, 0.707
θ range	1.89−25.99°	1.65−25.00°	2.30−23.26°
reflns collected	10 781	17 227	10 385
independent reflns	2786 [$R_{int} = 0.0528$]	8203 [$R_{int} = 0.0525$]	1590 [$R_{int} = 0.0561$]
data/restraints/param	2786/68/261	8203/523/439	1590/1/157
wR (F^2 all data)	wR2= 0.1221	wR2= 0.2991	wR2= 0.2147
R (F obsd data)	R1 = 0.0435	R1 = 0.1228	R1 = 0.0718
GOF on F^2	1.010	1.104	1.027
obsd data [$I > 2\sigma I$)]	2554	6996	1270
larg., mean shift (s.u.)	0.001, 0.000	0.000, 0.000	0.000, 0.000
larg. diff. peak, hole	0.926, −0.286 e/Å^3	1.621 and −1.031 e/Å^3	1.863 and −1.055 e/Å^3

1476, 1334, 1278, 1198, 1144, 1066, 935, 738, 688. Anal. Calcd for $C_{13}H_{20}N_4OS$: C, 55.69; H, 7.19; N, 19.98. Found: C, 56.02; H, 7.22; N, 19.91.

1-Methoxy-2-methyl-1,1-bis-(*N*-methyl-2-imidazolyl)-2-methylthiopropane (6b, 2-BIT^{NMe,OMe}). Sodium hydride (135 mg, 60% mineral oil suspension, 3.38 mmol) was suspended in dry THF (20 mL) under N_2. Compound **6a** (630 mg, 2.25 mmol) was dissolved in dry THF (10 mL) to give a colorless solution that was added dropwise to the NaH suspension over 2 min, and the resulting mixture was stirred for 1 h at rt until no bubbles appeared. Methyl iodide (210 μL, 3.38 mmol) was added dropwise and then the reaction mixture was stirred for 24 h. Then the reaction was quenched with 40 mL of deionized water and extracted twice with 25 mL portions of CH_2Cl_2, and the organic phase dried over $MgSO_4$. Rotary evaporation of the CH_2Cl_2 gave 400 mg of **6b** as a white solid (61%). ^{1}H NMR (300 MHz, $CDCl_3$): δ 1.70(s, 3H), 1.87(s, 6H), 3.13(s, 3H), 3.37(s, broad, 6H), 6.76(d, $J = 1.2$ Hz, 2H), 6.93(d, $J = 1.2$ Hz, 2H). ^{13}C NMR (75 MHz, $CDCl_3$): δ 146.3, 126.6, 123.2, 78.9, 56.7, 40.3, 34.3, 26.4, 12.9. HRMS (ESI) *m*/*z* 295.1580 (M + 1); calcd for $C_{14}H_{23}N_4OS$ 295.1593. IR (KBr; cm^{-1}): 2998, 2930, 1405, 1383, 1277, 1199, 1143, 1044, 935, 737, 669. Anal. Calcd for $C_{14}H_{22}N_4OS$: C, 57.11; H, 7.53; N, 19.03. Found: C, 57.31; H, 7.58; N, 18.94.

[(4-BIT$^{2\text{-Ph,NH,OH}}$)CuCO]PF$_6$ (7a). To **4a** (100 mg, 0.25 mmol) and $[Cu(CH_3CN)_4]PF_6$ (92 mg, 0.25 mmol) was added dry CH_2Cl_2 (6 mL), and the resulting light yellow solution was stirred at rt for 2 h under argon. Carbon monoxide was bubbled into the solution at rt for 1 h to give a cloudy solution. Compound **7a** was obtained as a white solid by slow diffusion of ether into the light yellow solution under N_2 (135 mg, 70%). IR (KBr; cm^{-1}): 3399, 2931, 2857, 2094, 1198, 1144, 1081, 843. ^{1}H NMR (300 MHz, CD_3OD): δ 1.28(s, 6H), 1.74(s, 3H), 5.48(s, 1H), 7.34(s, 2H), 7.50–7.60(m, 6H), 7.75–7.85(m, 4H). ^{13}C NMR (75 MHz, CD_3OD): δ 144.0, 131.4, 131.1, 130.5, 130.3, 128.5, 117.7, 76.6, 52.4, 24.8, 16.4. HRMS (ESI) *m*/*z* 495.0837; calcd for $C_{24}H_{24}{}^{63}CuN_4O_2S^+$ 495.0916.

[(4-BIT$^{2\text{-Ph,NMe,OH}}$)CuCO]PF$_6$ (8a). To **5a** (21 mg, 0.050 mmol) and $[Cu(CH_3CN)_4]PF_6$ (19 mg, 0.050 mmol) was added dry CH_2Cl_2 (5 mL), and the resulting light yellow solution was stirred at room temperature for 1 h under argon. Carbon monoxide was then bubbled into the solution at rt for 1 h to give a light yellow solution. Compound **8a** was obtained as a white solid by slow diffusion of ether into the solution at rt under N_2 (20 mg, 50%). IR (KBr; cm^{-1}): 3167, 2977, 2939, 2094, 1627, 1477, 1082, 838, 701, 559. ^{1}H NMR (300 MHz, CD_2Cl_2): δ 1.31(s, 6H), 1.80(s, 3H), 3.72(s, 6H), 7.31(s, 2H), 7.45–7.65(m, 10H). ^{13}C NMR (75 MHz, CD_2Cl_2): δ 144.0, 131.4, 131.1, 130.5, 130.3, 128.5, 117.7, 76.6, 52.4, 35.0, 24.8, 16.4. HRMS (ESI) *m*/*z* 523.1179; calcd for $C_{26}H_{28}{}^{63}CuN_4O_2S^+$ 523.1329.

[(2-BIT^{NMe,OMe})CuCO]PF$_6$ (9a′). To **6b** (30 mg, 0.10 mmol) and $[Cu(CH_3CN)_4]PF_6$ (38 mg, 0.10 mmol) was added dry CH_2Cl_2 (3 mL), and the resulting light purple solution was stirred at rt for 10 min under argon. Carbon monoxide was bubbled into the solution at for 0.5 h to give a light purple solution. Compound **9a′** was obtained as an off-white solid by slow diffusion of ether into the solution at rt under N_2 (40 mg, 59%). ^{1}H NMR (300 MHz, $CDCl_3$): δ 1.72(s, 3H), 1.94(s, 6H), 3.14(s, 6H), 4.08(s, 3H), 6.78(d, 2H), 6.96(d, 2H). ^{13}C NMR (75 MHz, $CDCl_3$): δ 145.3, 127.6, 122.2, 76.9, 54.7, 39.3, 30.3, 27.4, 14.9. HRMS (ESI) *m*/*z* 357.0822 calcd for $C_{14}H_{22}{}^{63}CuN_4OS^+$ 357.0810; 385.0810 calcd for $C_{15}H_{22}{}^{63}CuN_4O_2S^+$; 385.0859 found. IR (KBr; cm^{-1}): 3163, 3143, 2985, 2105, 1545, 1489, 1283, 1163, 1078, 878, 848, 774.

[(4-BIT$^{2\text{-Ph,NH,OMe}}$)$_2$Cu$_2$(OH)$_2$](PF$_6$)$_2$ (10). To **4b** (40 mg, 0.10 mmol) and $[Cu(CH_3CN)_4]PF_6$ (37 mg, 0.10 mmol) was added dry methanol (5 mL), and the resulting solution was stirred at rt for 1 h under argon. Then the solution was stirred under an O_2 atmosphere (balloon) at rt for 18 h to give a dark green solution. Green crystals of **10** were obtained by slow diffusion of ether into the solution over 6 days (60%). HRMS (ESI) *m*/*z* 497.0970 (8.6%), calcd for $C_{48}H_{52}{}^{63}Cu_2N_8O_4S_2{}^{2+}$, 497.1072; 497.5946(4.0%);

498.1057(21.7%), calcd for $C_{48}H_{54}{}^{63}Cu_2N_8O_4S_2{}^{2+}$, 498.1150; 498.6167(2.0%); 499.1148(5.0%). IR (KBr; cm^{-1}): 3387, 2932, 2855, 1700, 1652, 1559, 1459, 1077, 845. UV–vis(CH_3OH): 327 nm (ϵ 6.03 $\times$ 10^3 M^{-1} cm^{-1}). See X-ray experimental (Table 3) and Supporting Information for crystallographic data on **10**.

[(4-BIT$^{2\text{-Ph,NMe,OMe}}$)$_2$Cu$_2$(OH)$_2$](PF$_6$)$_2$ (11). To **5b** (10 mg, 0.020 mmol) and $[Cu(CH_3CN)_4]PF_6$ (8 mg, 0.020 mmol) was added dry CH_2Cl_2 (3 mL), and the resulting solution was stirred at rt for 1 h under argon. The solution was cooled to −50 °C, and then O_2 was bubbled into it. The colorless solution turned green within 5 min and was stirred under O_2 at −50 °C for 20 h. Green crystals of **11** were obtained by slow diffusion of ether into the green solution at room temperature (70%). HRMS (ESI) *m*/*z* 525.1569 (30%), calcd for $C_{52}H_{60}{}^{63}Cu_2N_8O_4S_2{}^{2+}$, 525.1486; 525.6665 (9.3%); 526.1510 (64%), calcd for $C_{52}H_{62}{}^{63}Cu_2N_8O_4S_2{}^{2+}$ 526.1564; 526.6640 (14%); 527.1560 (26%); 527.6537 (8.1%). IR (KBr; cm^{-1}): 3425, 2938, 2855, 1688, 1676, 1656, 1545, 1207, 1083, 842, 670, 558. UV–vis(CH_2Cl_2): 327 nm (ϵ = 6.03 $\times$ 10^3 M^{-1} cm^{-1}), 540 nm (ϵ = 281 M^{-1} cm^{-1}). See X-ray experimental (Table 3) and SI for crystallographic data on **11**.

[(2-BIT$^{\text{NMe,OMe}}$)$_2$Cu$_2$(OH)$_2$](PF$_6$)$_2$ (12). To **6b** (30 mg, 0.10 mmol) and $[Cu(CH_3CN)_4]PF_6$ (38 mg, 0.10 mmol) was added dry CH_2Cl_2 (5 mL), and the resulting solution was stirred at rt for 10 min under argon. The solution was cooled to −70 °C, and then O_2 was bubbled into it. The colorless solution turned blue within 2–3 min and was stirred under O_2 at −50 °C for 1 h to give a blue cloudy solution. After addition of 3 mL of methanol, the solution turned clear and dark blue. Needlelike blue crystals of **12** were obtained by slow diffusion of ether into the solution at rt (70%). LRMS(ESI, MeOH) *m*/*z* 388.11 (100.0%, for $C_{15}H_{25}{}^{63}CuN_4O_2S^+$), 390.10 (44.6%, for $C_{15}H_{25}{}^{65}CuN_4O_2S^+$). IR (KBr; cm^{-1}): 3429, 2931, 1547, 1494, 1283, 1164, 1080, 842, 758, 558. UV–vis (CH_3OH): λ 370 nm (ϵ 86.3 M^{-1} cm^{-1}). See X-ray experimental (Table 3) and SI for crystallographic data on **12**.

Computational Studies. PM3 and DFT computations were carried out using the Spartan 04 software suite (Wave function, Inc.). The energetically minimized structures (shown) were determined in the semiempirical PM3 mode, followed by single energy point calculations with the DFT method (B3LYP with 6–31G basis set and BP with 6–31G** basis set) to provide final calculated energies for comparison. A summary of the calculated Cartesian coordinates, energies and electrostatic charges for **13**−**18** is provided in the Supporting Information.

Acknowledgment. We are grateful for partial support of this project by the American Chemical Society Petroleum Research Fund. We also appreciate helpful discussions with Profs. R. Wheeler, R. Houser, and G. Richter-Addo. X-ray structure determinations by Dr. Douglas Powell and the assistance of the Richter−Addo group for the electrochemical experiments are also greatly appreciated.

Supporting Information Available: Cyclic volatammetric data for **1a′**, **7b′**−**9b′**, X-ray crystallographic data and analysis for **10**, **11**, and **12**, and PM3 and DFT computational output (Cartesian coordinates, calculated energies, and electrostatic charges) for **13**−**18**. This material is available free of charge via the Internet at http://pubs.acs.org.

IC800007T